

Submitted:
16.10.2020
Accepted:
04.02.2021
Published:
08.03.2021

Anatomical variations and interconnections of the superior peroneal retinaculum to adjacent lateral ankle structures: a preliminary imaging anatomy study

Eleni E. Drakonaki¹, Khaldun Ghali Gataa^{2,3},
Nektarios Solidakis^{2,3}, Pawel Szaro^{2,3,4}

¹ *Musculoskeletal Radiology Practice, Heraklion Crete Greece & Medical School, European University of Cyprus, Cyprus*

² *Department of Musculoskeletal Radiology, Sahlgrenska University Hospital, Sweden*

³ *Department of Radiology, Institute of Clinical Sciences, Sahlgrenska Academy, University of Gothenburg, Sweden*

⁴ *Department of Clinical and Descriptive Anatomy, Medical University of Warsaw, Poland*

Correspondence: Dr Pawel Szaro, e-mail: pawel.szaro@gu.se

DOI: 10.15557/JoU.2021.0003

Keywords

ultrasonography,
ankle,
ligament,
connections,
retinaculum

Abstract

Aim: This imaging anatomy study aimed at detecting anatomical variations and potential interconnections of the superior peroneal retinaculum to other lateral stabilizing structures. **Materials and methods:** We retrospectively reviewed the imaging archives of 63 patients (38 females, 25 males, mean age 32.7, range 18–58 years) with available ankle US, MR and CT images to detect whether US and MR can detect the presence of interconnections between the superior peroneal retinaculum and the anterior talofibular ligament, inferior extensor retinaculum and peroneal tendon sheath. We evaluated the presence of common anatomical variations including low peroneus brevis muscle belly, peroneal tubercle, os peroneum, and retromalleolar fibular groove shape in relation to the presence of superior peroneal retinaculum connections. **Results:** The connections of the superior peroneal retinaculum can be revealed on magnetic resonance imaging (MRI) and ultrasound (US). The connection to the anterior talofibular ligament was located (a) inferior to the lateral malleolus, (b) at the level of the lateral malleolus and (c) on both levels, respectively (a) 49.2% on MRI and 39.7% on US, $p < 0.05$, (b) 44.4% and 58.7%, $p < 0.05$, 36.5% and (c) 27%, $p < 0.05$. Superior peroneal retinaculum–inferior extensor retinaculum (MRI 47.6%, US 28.6% $p < 0.001$) and superior peroneal retinaculum–peroneal tendon sheath (MRI 22.2%, US 25.4% $p > 0.05$) connections were also found both on MR and US. **Conclusion:** Ankle US and MR revealed interconnections between the superior peroneal retinaculum and the anterior talofibular ligament, inferior extensor retinaculum, and superior peroneal retinaculum. Our results are a starting point for further studies on the connections of the superior peroneal retinaculum and the applicability of ultrasound and MRI in assessing their occurrence. Knowledge of the anatomical connections of the superior peroneal retinaculum may help radiologists with the assessment of lateral ankle injuries, and surgeons with treatment planning.

Introduction

The peroneal retinacula are fibrous retaining bands that stabilize the peroneal tendons at the malleolar groove^(1,2). The superior peroneal retinaculum (SPR) is a complex structure forming the retromalleolar fibular groove's

posterolateral border. Anatomical variations, including the retromalleolar fibular groove shape, trochlear tubercle, os peroneum, and low-lying peroneus brevis muscle belly, may contribute to peroneal tendon disorders^(1,3–5). Moreover, injuries of the SPR commonly coexist with lateral ankle ligament injury^(3,6–8). The posttraumatic lateral ankle pain

is frequently caused by lateral ankle instability. Chronic lateral ankle instability may be caused by the laxity of the SPR, which may result in peroneus brevis split rupture⁽⁹⁾. There is no sufficient anatomical background for the cited clinical observation. The presence of a concomitant injury of the lateral ankle ligament results from the mechanism of injury and is probably related to interconnections between ligaments^(10,11). Connections of the SPR with ligaments in the Kager's fat pad were previously revealed⁽¹²⁾. The SPR was connected most commonly with the fibulotalocalcaneal ligament, the paratenon, the posterior talofibular ligament, the flexor retinaculum, and the anterior talofibular ligament (ATFL)⁽¹²⁾.

High-resolution magnetic resonance (MR) imaging using 1.5 T and high-resolution ultrasonography (US) with high-frequency linear transducers allow detailed delineation of the anatomy and diseases of the lateral ankle structures, including the SPR^(13,14). Various MR studies have evaluated the appearance of the SPR and variations of the peroneal tendon complex^(1,5,14-17). Using MR imaging, interconnections have been reported between the following structures: the anterior talofibular ligament (ATFL), the inferior extensor retinaculum (IER), and the peroneal tendon sheath (PTS), and their association to other common anatomical variations described in the literature^(11,12,18,19). Interconnections of the SPR to the lateral ankle structures have not been previously reported on US, and limited literature is available using MR⁽¹²⁾.

The research hypothesis was that the connections between the SPR and the neighboring structures are visible in ankle ultrasound.

Material and methods

This is a retrospective study of 63 patients with available ankle US, CT, and MR images (38/25 females/males, mean age 32.7, range 18–58 years). All examinations were performed as part of the clinical routine from July 2018 to November 2019. The findings were reviewed twice, and the final decision was made by consensus.

The inclusion criteria were a non-traumatic indication, availability of complete US videos, at least T2- or PD (proton density)-weighted MR sequences without fat suppression in the axial plane, and ankle CT. The exclusion criteria comprised a history of fracture (12 cases), obvious abnormality in the lateral ankle region such as tumor or inflammation (5 cases), presence of orthopedic hardware (7 cases), and low US video quality (4 cases). In total, 63 patients fulfilled the criteria and were included in the study group.

MR examinations were performed using the Ingenia 3.0T MR system (Philips Healthcare) with a dedicated ankle coil. PD TSE (turbo spin-echo) in the axial plane: TE (echo time) 45 ms, TR (repetition time) 2800–5000 ms, FOV (field of view) 14 cm. T2 TSE in the axial plane: TE 80 ms, TR 3000–5000 ms, FOV 14 cm. US examinations were performed using the GE Logiq 9 system with 6–15 MHz and 8–18 MHz probes. CT examinations were conducted using cone-beam or 256-slice scanners.

We assessed anatomical interconnections between the SPR and the ATFL, PTS, and IER. The interconnections were considered present on MR and/or US, respectively, when thin, linear, low signal intensity bands were evident and/or when thin isoechoic or hyperechoic linear fibrillar structures were found between the above structures. We assessed the presence of connections first on US and then MR images. MR assessment. Firstly, the SPR was found on the horizontal sections based on the anatomical location. We then assessed where the SPR ended by analyzing subsequent cross-sections, and determined whether there was a clear difference between the SPR, which was considered an absent connection. The observations were confirmed on the frontal images on MRI and other projections on ultrasound.

Anatomical variations including the os peroneum, peroneal tubercle, retromalleolar fibular groove shape variation, low-lying peroneus brevis muscle, peroneus tertius, and quartus muscles were assessed on US images. Verification of soft tissue variants was performed on MR and bone variants on CT images, based on previously described criteria⁽¹⁾. The

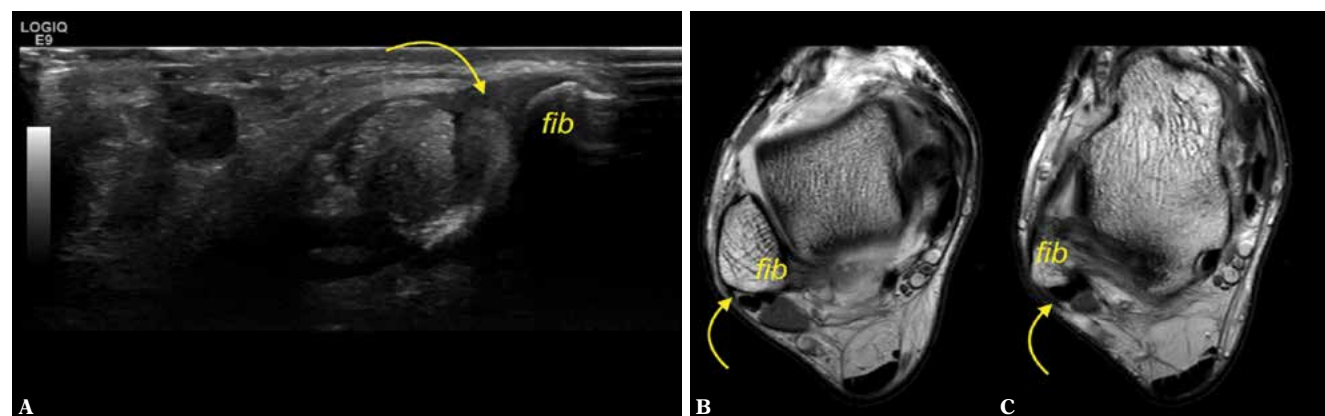


Fig. 1. A 19-year-old patient with a clinical suspicion of rheumatoid arthritis. **A.** ultrasound, transverse section. **B, C.** proton density-weighted transverse sections. *Fib* – fibula. *SPR* – curved arrow. No connection with IER is present

Tab. 1. Interconnections between the SPR, ATFL, IER, and PTS revealed on ultrasound and MRI, $N = 63$. P -values indicated as * $p < 0.05$ and ** $p < 0.001$

| | ATFL – SPR at the level of lateral malleolus | ATFL – SPR inferior to lateral malleolus | ATFL – SPR at the level and inferior to the lateral malleolus | SPR – IER | SPR – PTS |
|------------|----------------------------------------------|------------------------------------------|---------------------------------------------------------------|-----------|-----------|
| US | 37 | 25 | 17 | 18 | 16 |
| | 58.7% | 39.7% | 27.0% | 28.6% | 25.4% |
| MRI | 28 | 31 | 23 | 30 | 14 |
| | 44.4% | 49.2% | 36.5% | 47.6% | 22.2% |
| Difference | 14.3%* | 9.5%* | 9.5%* | 19.0%** | 3.2% |

Tab. 2. Prevalence of variants of the retro-malleolar fibular groove, peroneal tubercle, and os peroneum. $N = 63$. P -values indicated as * $p < 0.05$

| | | Retromalleolar fibular groove shape | | | Presence of peroneal tubercle | Presence of os peroneum |
|------------|-----|-------------------------------------|-------|--------|-------------------------------|-------------------------|
| | | concave | flat | convex | | |
| US | n | 39 | 14 | 10 | 41 | 3 |
| | % | 61.9% | 22.2% | 15.9% | 65.1% | 4.8% |
| CT | n | 45 | 12 | 6 | 40 | 6 |
| | % | 71.4% | 19.0% | 9.5% | 63.5% | 9.5% |
| Difference | % | 9.5%* | 3.2%* | 6.3% | 1.6%* | 1.6% |

retromalleolar fibular groove shape was characterized in line with the standard criteria as flat, convex, or concave⁽¹⁾. The definition of hypertrophy of the peroneal tubercle was applied from previous studies as the tubercle projecting beyond the outer contour of the peroneal tendons⁽²⁰⁾.

Statistical analysis was performed using SPSS 8.0. To compare the prevalence of connections between US and MR, a chi-square test was used. The level of statistical significance was set at $p < 0.05$.

The Ethics Committee approved the study and waived the need for informed consent (number 2020-06177). The study was conducted in compliance with the Declaration of Helsinki. The anonymization of patient data ensured data protection following the European General Data Protection Regulation. The data were recorded in a password-protected secure database.

Results

The SPR was found to be connected to at least one of the examined lateral structures in 16 cases (25.3%) on US, and in 14 cases (22.2%) on MR, whereas no connections at all were identified in 6 cases (9.5%) on MR and 3 cases (4.8%) on US; the differences are not statistically significant ($p > 0.05$). When the SPR did not extend beyond the outer outline of the lateral malleolus, connections were considered absent (Fig. 1). The SPR connections are shown in Tab. 1 and other anatomical variations in Tab. 2.

Superior peroneal retinaculum – anterior talofibular ligament

This was the most common connection seen on US. Interconnections between the SPR and ATFL were found between the lateral malleolus level and the area inferior to it (Fig. 2, Tab. 1). The most common variant of the

SPR-ATFL connection on MR was located inferior to the lateral malleolus tip ($n = 31$, 49.2%). The connections that were significantly more often detectable on MR than US are located inferiorly to the lateral malleolus (49.2% vs 39.7%, $p < 0.05$) and at the level of the lateral malleolus and inferior to it (36.5% vs. 27%, $p < 0.05$). The presence of connections at the lateral malleolus level was noted significantly more commonly on US than on MRI (58.7% vs. 44.4% $p < 0.05$).

Superior peroneal retinaculum – inferior extensor retinaculum

MR revealed this connection significantly more often than US (47.6% vs. 28.6%, $p < 0.001$) (Tab. 1). The connection was visualized as a linear echogenic fibrous band on US, and as a narrow, low signal intensity linear strip on MR, and was often evident at the external outline of the lateral malleolus near the cortex (Fig. 3 and Fig. 4).

The IER served as an intermediate station for connecting the SPR to the ATFL in 8 cases on MRI (12.7%) and in 5 cases on US (7.9%), but the difference was not significant ($p > 0.05$) (Fig. 3). In those cases, a direct connection between the SPR and the ATFL was also noted ($n = 13$, 20.6%) (Fig. 5).

Superior peroneal retinaculum – peroneal tendon sheath

Connections to the PTS were found in 25.4% cases on US and 22.2% on MR. They were located inferior to the apex of the lateral malleolus (Fig. 6). The difference in the frequency of this connection between MR and US was the smallest among all the connections (difference 3.2%, $p > 0.05$) (Tab. 1).

There were no statistically significant differences in the number of SPR connections between the group of males and females or body sides ($p > 0.05$).

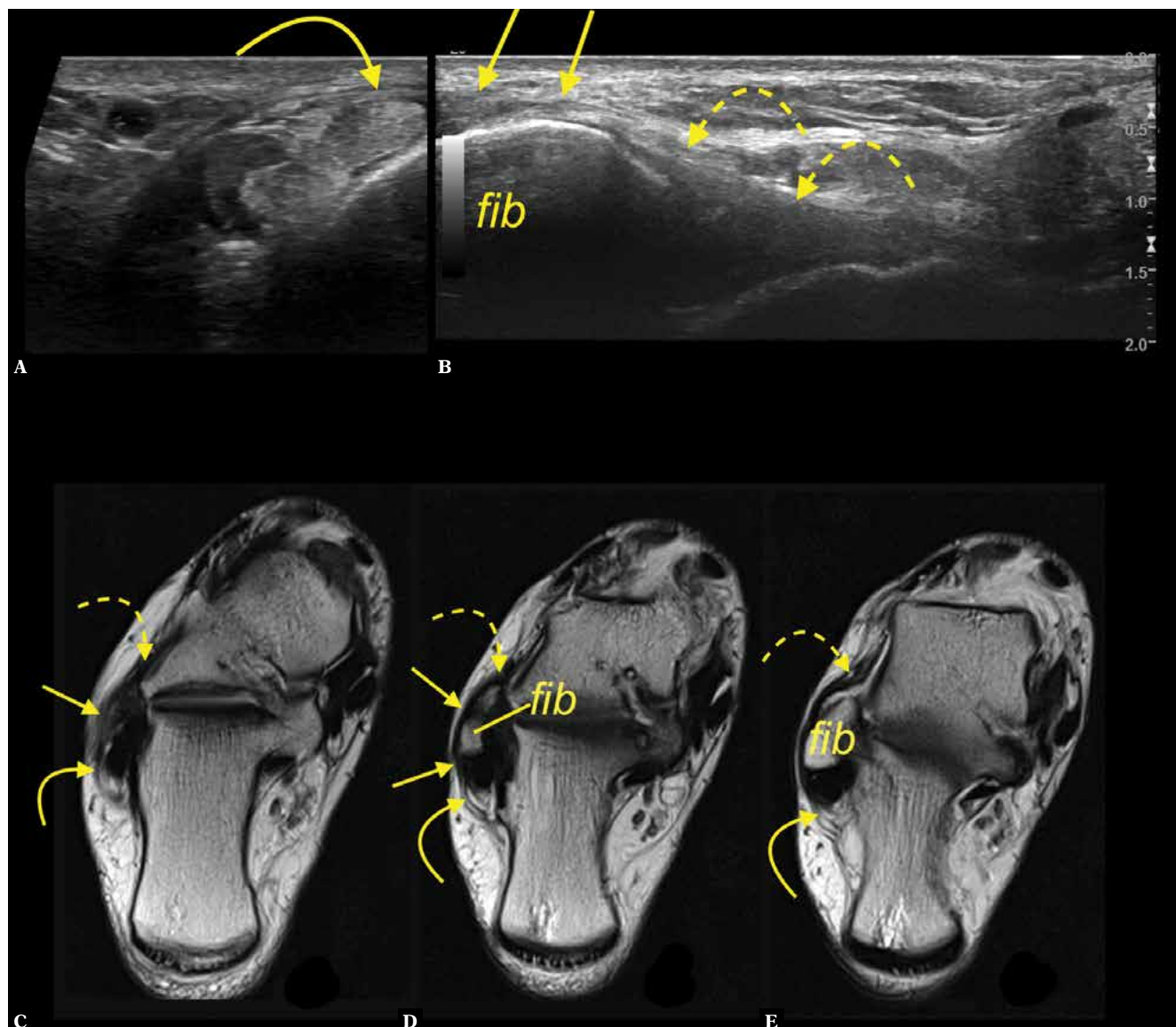


Fig. 2. A 34-year-old patient with a suspicion of a ganglion. **A, B.** transverse section on ultrasound corresponding to section **d**. **C, D, E.** T2-weighted slightly oblique section. The interconnection (straight arrows) between the SPR (curved arrow) and ATFL (curved dashed arrow); fib – fibula

Other anatomical variations

The concave shape was the most common anatomical variant of the retromalleolar fibular groove, found on CT in 71.4% and on US in 61.9%, ($p < 0.05$) cases, followed by flat (CT in 19% and US in 22.2%, $p < 0.05$) and convex shapes (CT in 9.5% and US in 15.5%, $p > 0.05$) (Tab. 2, Fig. 7). More flat and convex cases were revealed on US than on CT, yet the difference was statistically significant only for the flat shape. Statistically significant differences in the presence of connections between the SPR and the ATFL were noticed only for the concave type of retromalleolar fibular groove in MRI assessment (Tab. 3).

In most cases, the peroneal tubercle was found both on US and CT (65.1% and 63.5%, respectively) (Tab. 2, Fig. 8); however, no hypertrophy of the peroneal tubercle was

observed. US showed the peroneal tubercle presence in 1.6% cases more compared to CT ($p < 0.05$). We identified 6 cases (9.5%) with os peroneum present on CT while only 3 (4.8%) of them were detected on US ($p > 0.05$). Low-lying peroneus brevis muscle belly was identified in 7 cases (11.1%) on US and in 5 cases on CT (7.9%), $p < 0.05$. No case of peroneus quartus or tertius muscle was found.

Discussion

The most important finding of this paper is that SPR connections to the adjacent structures exist and can be visualized on MR and US. The most common SPR connection found on US was that with the ATFL, followed by the connection with the IER and PTS. The most common connection evident on MR was that to the IER, followed by the ATFL and PTS. The IER,

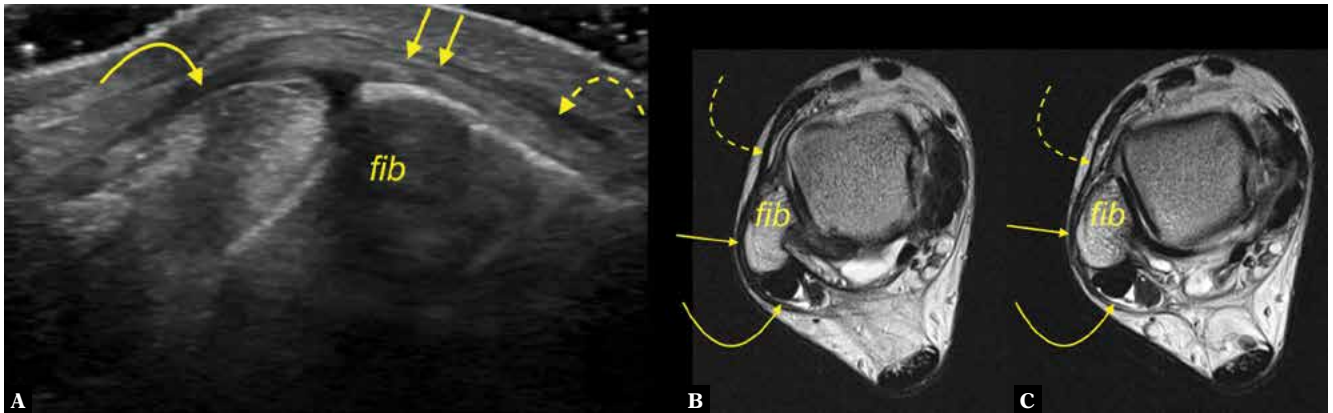


Fig. 3. A 24-year-old patient with pain anterior to the lateral malleolus. **A.** transverse section on ultrasound, **B, C.** T2-weighted slightly oblique sections. The interconnection (arrows) between the SPR (curved arrow) and IER (dashed arrow); fib – fibula

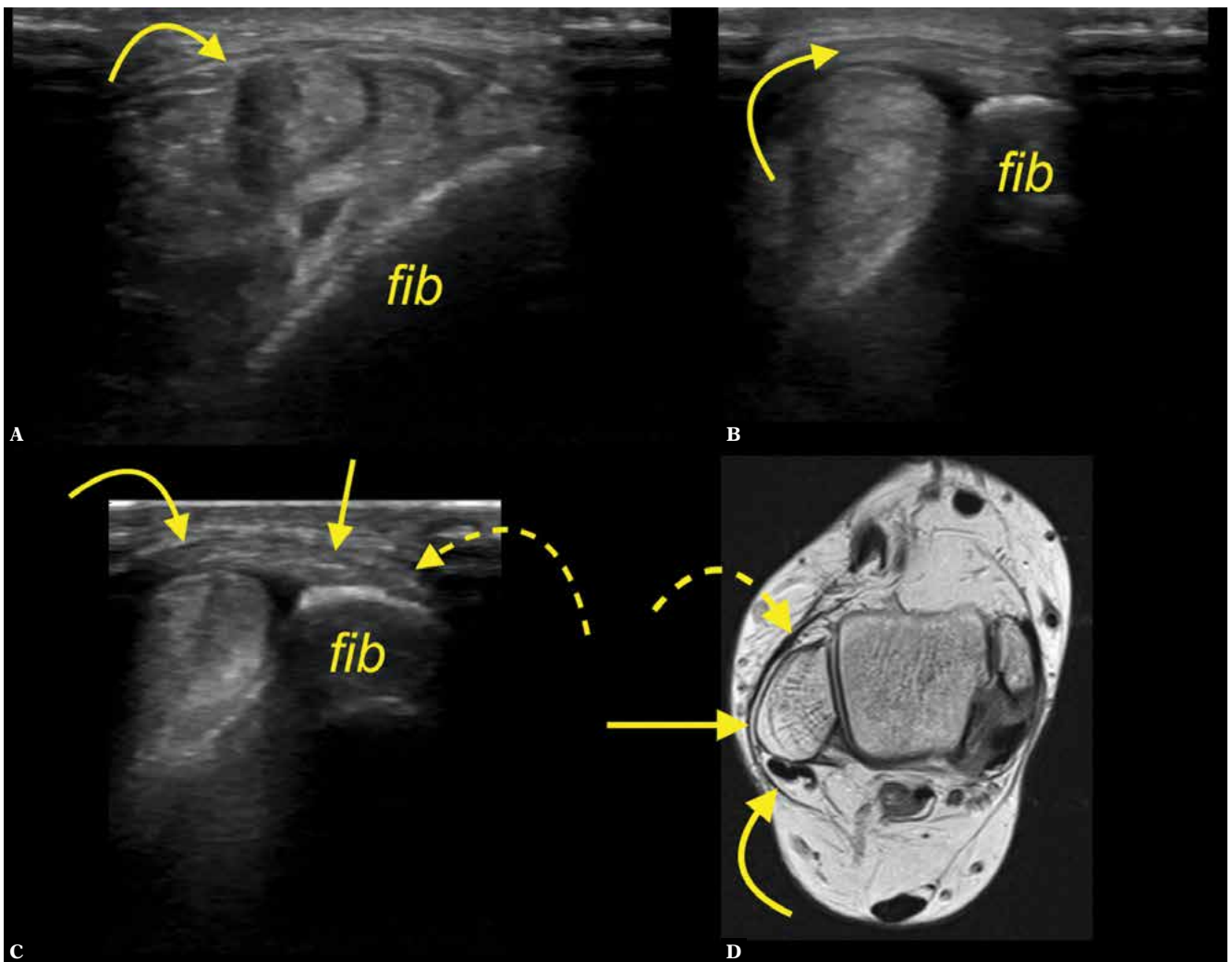


Fig. 4. A 42-year-old patient presenting clinical suspicion of synovitis. **A, B, C.** transverse section on ultrasound, **d.** proton density-weighted oblique oriented section. The interconnection (arrows) between the SPR (curved arrow) and IER (dashed arrow); fib- fibula

due to its location, was found to serve as an intermediate station for connecting the SPR to the ATFL. These imaging studies confirm previous findings regarding lateral ankle ligament interconnections reported in cadaveric studies^(18,21) and

MRI⁽¹¹⁾. The SPR connection to the calcaneofibular ligament and the Achilles paratenon was reported previously both in cadavers and MR imaging studies^(12,21). Other variations have been previously reported in cadavers, including the inferior

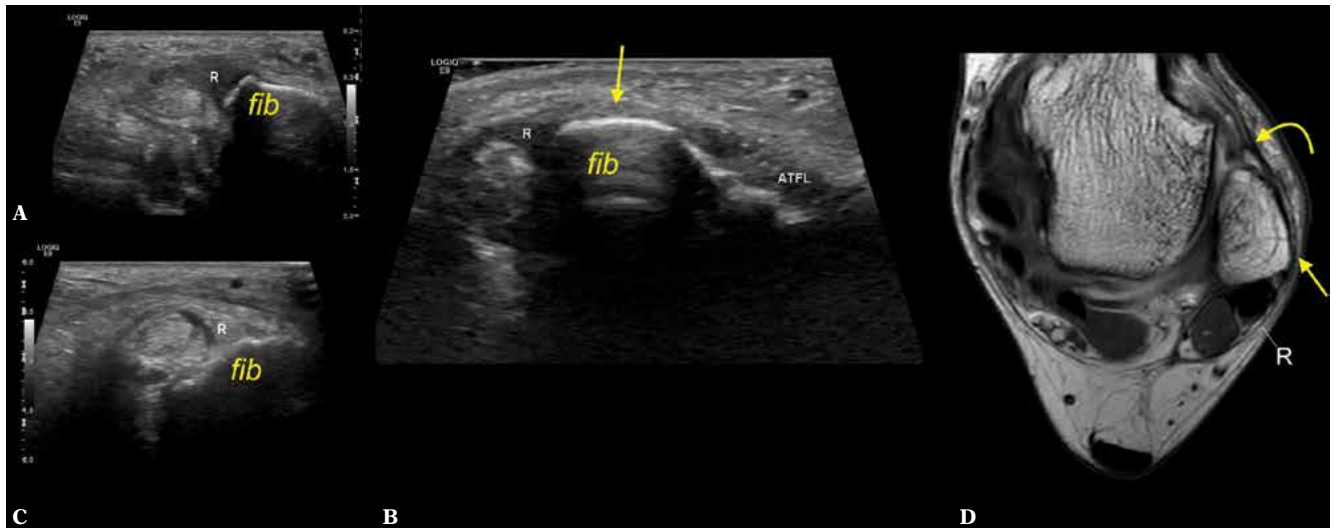


Fig. 5. A 52-year-old patient presented with retromalleolar pain. **A, B, C.** transverse section on ultrasound. **D.** proton density-weighted transverse section. The interconnection (arrows) between the SPR (letter R) and IER (curved arrow) and ATFL. Fib – fibula

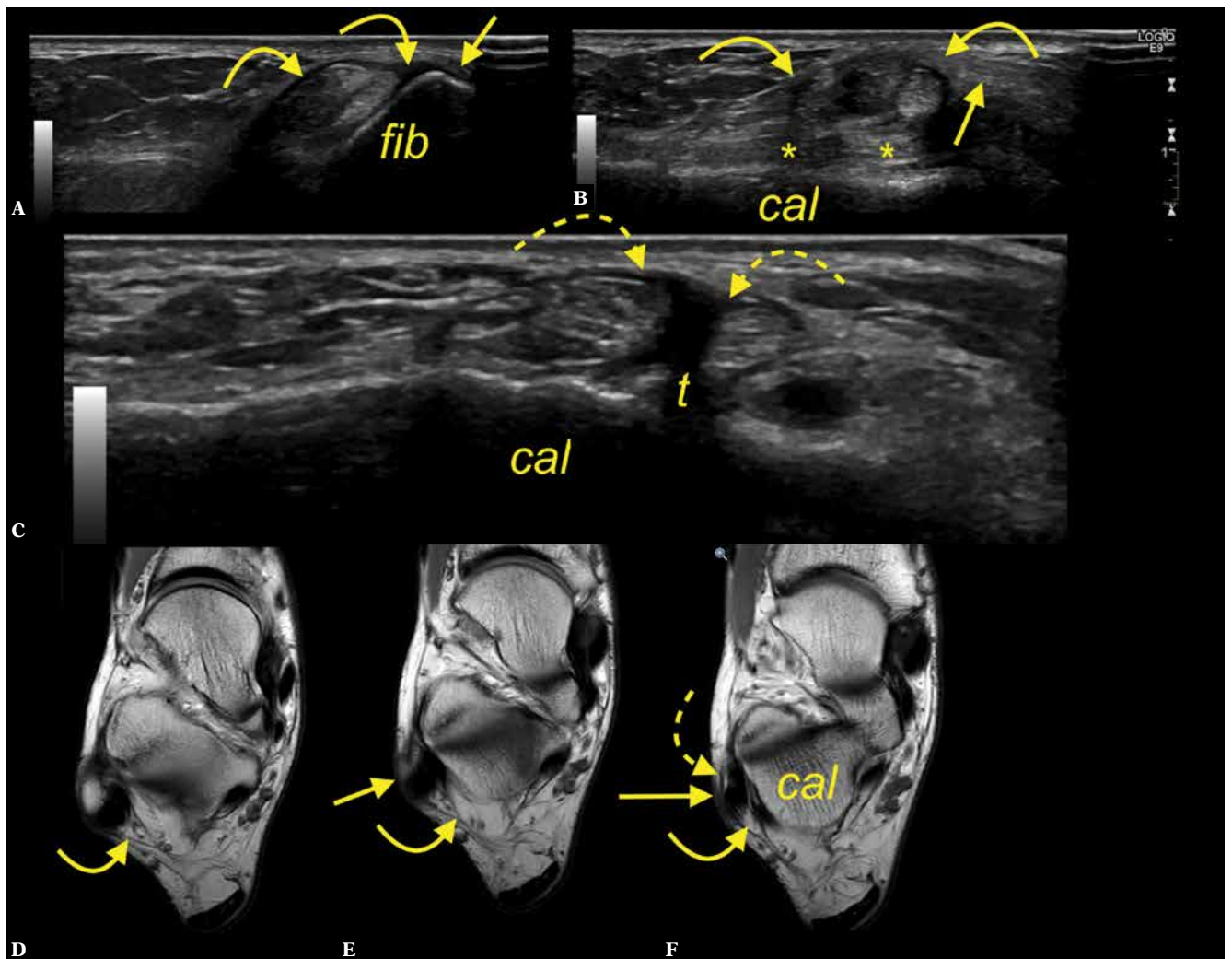


Fig. 6. A 28-year-old patient with a clinical suspicion of an intraarticular free body in the ankle joint. **A.** transverse section at the level of the lateral malleolus (fib – fibula), SPR – curved arrow, connection to the PTS (straight arrow). **B.** oblique section along the calcaneofibular ligament (asterisk). **C.** coronal section at the level of the peroneal tubercle (t), PTS – dashed arrow, calcaneus – cal. **D, E, F.** MRI proton density-weighted axial sections

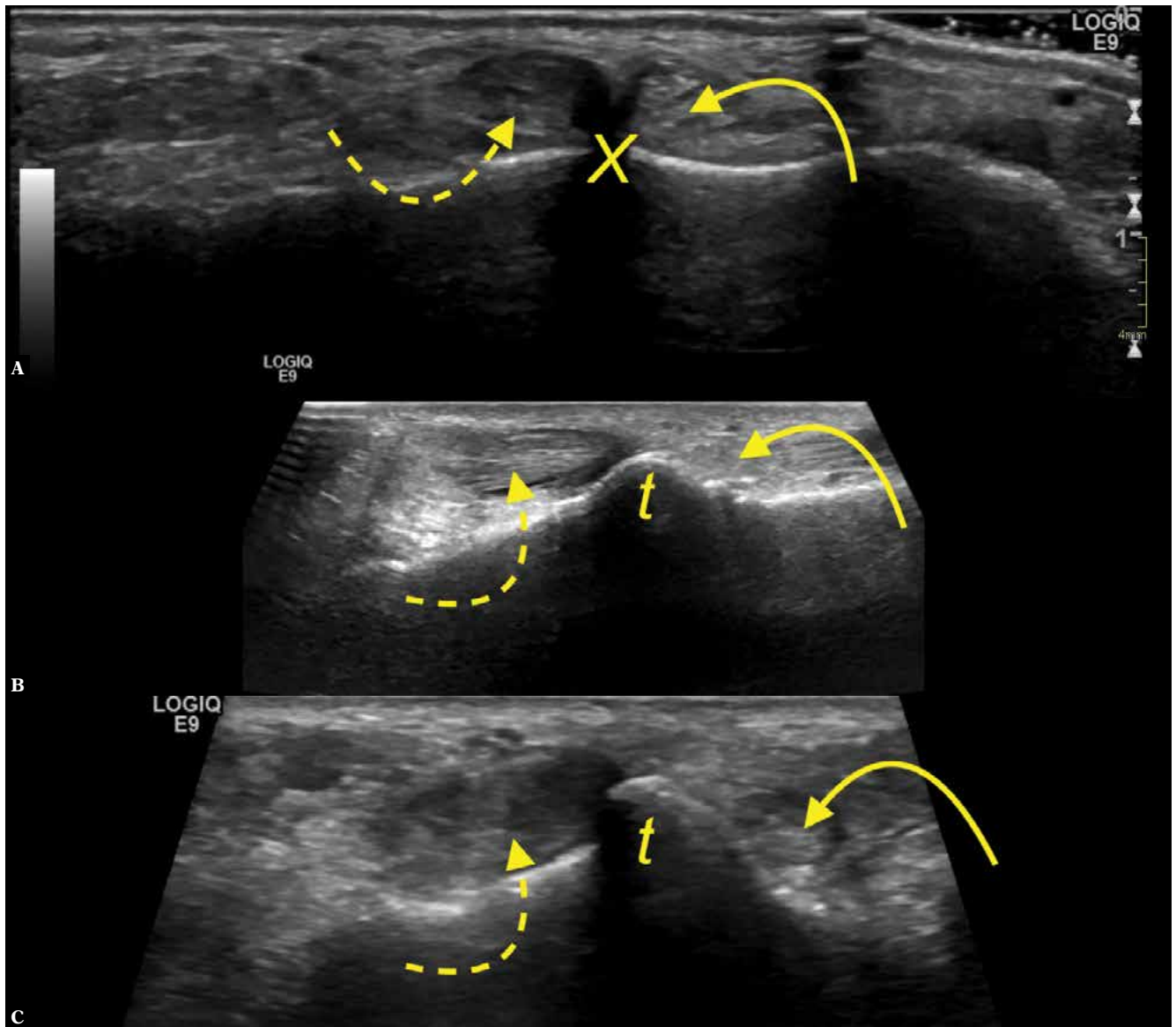


Fig. 7. Anatomical variations of the peroneal tubercle, three different patients. **A, B, C.** coronal sections, ultrasound, **A.** no explicit peroneal tubercle was noted (X), **B, C.** the peroneal tubercle (t) was present. The peroneus brevis (curved arrow) and the peroneus longus (dashes curved arrow)

Tab. 3. Differences in the presence of interconnections between different variants of retromalleolar fibular groove on US and MRI, p-value

| Modality | Variant of retromalleolar fibular groove | ATFL-SPR at the level of lateral malleolus | ATFL-SPR inferior to lateral malleolus | ATFL-SPR at the level and inferior to lateral malleolus | SPR-IER | SPR-PTS |
|----------|------------------------------------------|--------------------------------------------|----------------------------------------|---------------------------------------------------------|---------|---------|
| US | convex | 0.80 | 0.42 | 0.55 | 0.38 | 0.59 |
| | concave | 0.26 | 0.31 | 0.36 | 0.82 | 0.79 |
| | flat | 0.69 | 0.95 | 0.70 | 0.43 | 0.81 |
| CT | convex | 0.23 | 0.14 | 0.11 | 0.45 | 0.66 |
| | concave | <0.05 | <0.05 | <0.05 | 0.53 | 0.26 |
| | flat | 0.20 | 0.09 | 0.18 | 0.54 | 0.31 |

peroneal retinaculum’s connection to the lateral calcaneal process⁽²²⁾ or the IER⁽²³⁾. These findings probably indicate a tendency for the lateral structures to interconnect and form larger functional units. The tendency to developing the connections between structures was also observed in the medial

area of the ankle. The flexor retinaculum connections with the deltoid ligament, the fibulotalocalcaneal ligament, and the flexor fibrous sheath were reported previously⁽²⁴⁾. To our knowledge, the connections found in our study have not been previously described in US, cadaveric or surgical studies.

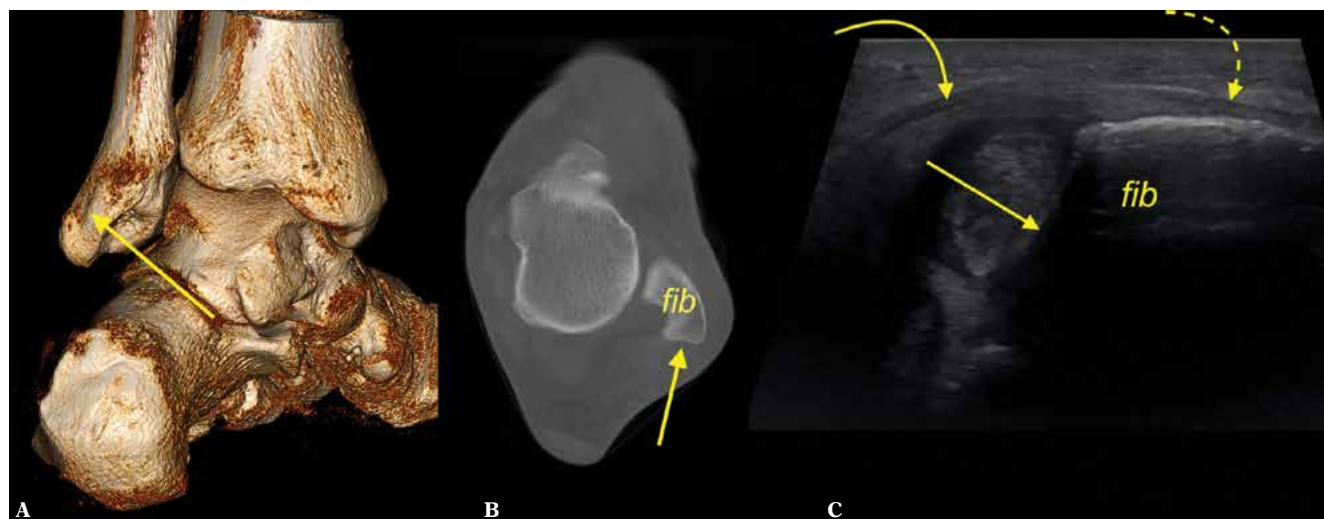


Fig. 8. The most common variant of the retromalleolar fibular groove, convex (straight arrow). A 39-year-old patient with a suspicion of rheumatoid arthritis. **A, B.** cone-beam computed tomography (**A.** 3D posterior medial view, **B.** transverse section), **C.** transverse ultrasound section. SPR (curved arrow) was connected (dashed curved arrow) to IER (not shown). Fib – the lateral malleolus

MR has been proved useful for the assessment of foot retinacula^(15,25,26). Additionally, MR is not affected by overdissection, which is a common problem in anatomical research. However, there is scarce evidence on the existence of these connections in MR studies. In a previous MR study, we documented SPR connections to the fibulotalocalcaneal ligament, the posterior talofibular ligament, and the flexor retinaculum via the fibulotalocalcaneal ligament⁽¹²⁾. The SPR-ATFL connection in that study was found in only 9% of cases, which is a lower proportion than in the current study.

SPR connections are essential components of a functional complex at the lateral malleolus level^(12,27). Statistically significant differences in the occurrence of connections revealed on MRI between the ATFL and PTS were noticed before between groups of single and double fascicular ATFL and CFL⁽¹¹⁾. It is challenging to distinguish between single and double fascicular ATFL on US; thus, comparing the results is not entirely possible, which is a limitation of this study.

MR showed significantly more SPR connections than US in all cases except the ATFL-SPR connection located at the lateral malleolus level, and the SPR-PTS connection. This observation indicates the complementary roles of MR and US. The slightest difference between MR and US was encountered for the SPR-PTS connection, and the greatest for the SPR-IER connection. The discrepancies between MR and US may be due to technical issues, mostly affecting the US examination. The SPR is best imaged on US in the axial oblique plane, and the degree of transducer obliquity depends on the course of the retinaculum, which differs widely among patients, and the operator's skills to identify the correct plane^(13,14). Those parameters may result in poor US visualization of the SPR and reduced possibility of identifying the associated connecting fibers.

Moreover, the lack of contrast between the echogenic connecting fibers and the surrounding subcutaneous fat may

be another reason for the US's lower sensitivity. On the contrary, the contrast between the fat and fibrous tissue is excellent on MR, allowing the connecting fibrous bands to be easily identified. Interestingly, US was found to reveal more SPR-ATFL connections at the lateral malleolus level than MR. This may be attributed to the fact that the fibers connecting superficially to the lateral malleolus are more clearly delineated on US than MR, where the low signal fibers blend with the low signal of the cortical bone, limiting the discrimination between them⁽²⁸⁾.

The results of our study may have important clinical implications. These connections may explain various combinations commonly encountered in lateral ankle instability patterns^(3,6-8,29). It has been suggested that a disruption of the lateral collateral ligaments induces strain and injury on the SPR, which may explain why the conditions commonly coexist⁽⁸⁾. Our findings suggest the presence of an anatomical (besides the biomechanical) connection between the SPR and ATFL. This study's findings could be clinically relevant to radiologists in routine assessment of SPR connections in lateral ankle sprains and surgeons for planning reconstruction procedures.

We also assessed the presence of other anatomical variations which may influence the functions of the peroneal tendons. The incidence of the peroneal tubercle and os peroneum found in our study is comparable to the values reported in the literature. The incidence of the peroneal tubercle is estimated at 40–84%, and os peroneum at 7–20%^(1,30). The low-lying peroneus brevis muscle belly was less common in our study than in previous studies, where it was reported to range between 23.2% and 87%^(30,31). However, the level of the muscle belly changes with foot position⁽³²⁾, and it is challenging to identify the retromalleolar fibular groove on US, which may explain the reported differences. The retromalleolar fibular groove's concave shape was the most common variant, followed by flat and convex shapes. The finding is in agreement with prior studies reporting a cadaveric incidence of 68–82% for the concave type^(1,33); however, in other

studies, the convex or flat shape was shown to be the most common^(30,34,35). Such differences may represent epidemiological, ethnic or developmental variation. It is difficult to determine whether the variants of the retromalleolar fibular groove may be related to the presence of SPR connections, but the developmental background may be possible.

Considering CT as the appropriate bone surface rendering method, we found that US underestimated the concave shape, while overestimating the flat and convex shape frequencies. US also overestimated the incidence of the peroneal tubercle compared to CT. These differences may be attributed to variations in the scanning planes and operator dependency, making CT imaging a more reproducible method for assessing bone morphology than US.

This study has its limitations. We are aware of the most important limitation of this study, namely the use of ultrasound in the context of a retrospective study. The method of minimizing this negative effect was the use of ultrasound films and MRI. The present study and its results are a starting point for further prospective work in ultrasound and MRI. The slice thickness in the MRI protocol was 3 mm, and no 3D sequences were available. Also, we had no surgical correlation for our findings.

References

- Wang XT, Rosenberg ZS, Mechlin MB, Schweitzer ME: Normal variants and diseases of the peroneal tendons and superior peroneal retinaculum: MR imaging features. *Radiographics* 2005; 25: 587–602.
- Athavale SA, Swathi, Vangara SV: Anatomy of the superior peroneal tunnel. *J Bone Joint Surg Am* 2011; 93: 564–571.
- Sobel M, Geppert MJ, Warren RF: Chronic ankle instability as a cause of peroneal tendon injury. *Clin Orthop Relat Res* 1993; 187–191.
- Mirmiran R, Squire C, Wassell D: Prevalence and role of a low-lying peroneus brevis muscle belly in patients with peroneal tendon pathologic features: a potential source of tendon subluxation. *J Foot Ankle Surg* 2015; 54: 872–875.
- Galli MM, Protzman NM, Mandelker EM, Malhotra AD, Schwartz E, Brigido SA: An examination of anatomic variants and incidental peroneal tendon pathologic features: a comprehensive MRI review of asymptomatic lateral ankles. *J Foot Ankle Surg* 2015; 54: 164–172.
- Alparslan L, Chiodo CP: Lateral ankle instability: MR imaging of associated injuries and surgical treatment procedures. *Semin Musculoskelet Radiol* 2008; 12: 346–358.
- Kirby AB, Beall DP, Murphy MP, Ly JQ, Fish JR: Magnetic resonance imaging findings of chronic lateral ankle instability. *Curr Probl Diagn Radiol* 2005; 34: 196–203.
- Ferran NA, Oliva F, Maffulli N: Recurrent subluxation of the peroneal tendons. *Sports Med* 2006; 36: 839–846.
- Sobel M, Geppert Mj Fau, Warren RF: Chronic ankle instability as a cause of peroneal tendon injury. *Clin Orthop Relat Res* 1993; 187–191.
- Dalmau-Pastor M, Malagelada F, Calder J, Manzanares MC, Vega J: The lateral ankle ligaments are interconnected: the medial connecting fibres between the anterior talofibular, calcaneofibular and posterior talofibular ligaments. *Knee Surg Sports Traumatol Arthrosc* 2020; 28: 34–39.
- Szaro P, Ghali Gataa K, Polaczek M, Ciszek B: The double fascicular variations of the anterior talofibular ligament and the calcaneofibular ligament correlate with interconnections between lateral ankle structures revealed on magnetic resonance imaging. *Sci Rep* 2020; 10: 20801.
- Szaro P, Polaczek M, Ciszek B: The Kager's fat pad radiological anatomy revised. *Surg Radiol Anat* 2021; 43: 79–86.

Conclusions

In conclusion, US and MRI evaluation may reveal interconnections between the SPR and the ATFL, IER, and PTS. The SPR may connect with other structures in relation to the lateral malleolus. Our results are a starting point for further prospective research in ultrasound and MRI. Our study confirms the complementary role of MR and US examinations in evaluating variable connections of the SPR. However, we see the need of future prospective studies focusing on the usefulness of ultrasound in assessing the presence of connections with correlation to MRI. Knowledge of the anatomical connections of the SPR may help radiologists with the assessment of lateral ankle injuries and assist surgeons in treatment planning.

Conflict of interest

None declared. The authors declare that this work has not received any funding before or during research. There are no relationships with any companies whose products or services may be related to the article's subject matter.

- Bianchi S, Delmi M, Molini L: Ultrasound of peroneal tendons. *Semin Musculoskelet Radiol* 2010; 14: 292–306.
- Taljanovic MS, Alcalá JN, Gimber LH, Rieke JD, Chilvers MM, Latt LD: High-resolution US and MR imaging of peroneal tendon injuries. *Radiographics* 2015; 35: 179–199.
- Numkarunarunrote N, Malik A, Aguiar RO, Trudell DJ, Resnick D: Retinacula of the foot and ankle: MRI with anatomic correlation in cadavers. *AJR Am J Roentgenol* 2007; 188: W348–354.
- Guo S, Yan YY, Lee SSY, Tan TJ: Accessory ossicles of the foot-an imaging conundrum. *Emerg Radiol* 2019; 26: 465–478.
- Yıldız D, Ekiz T, Doğan A: Lateral ankle pain and peroneal tendon subluxation in a patient with peroneal quartus muscle and superior peroneal retinaculum injury. *J Back Musculoskelet Rehabil* 2017; 30: 1147–1148.
- Vega J, Malagelada F, Manzanares Cespedes MC, Dalmau-Pastor M: The lateral fibulotalocalcaneal ligament complex: an ankle stabilizing isometric structure. *Knee Surg Sports Traumatol Arthrosc* 2020; 28: 8–17.
- Edama M, Kageyama I, Kikumoto T, Nakamura M, Ito W, Nakamura E *et al.*: Morphological features of the anterior talofibular ligament by the number of fiber bundles. *Ann Anat* 2018; 216: 69–74.
- Saupe N, Mengiardi B, Pfirrmann CW, Vienne P, Seifert B, Zanetti M: Anatomic variants associated with peroneal tendon disorders: MR imaging findings in volunteers with asymptomatic ankles. *Radiology* 2007; 242: 509–517.
- Davis WH, Sobel M, Deland J, Bohne WH, Patel MB: The superior peroneal retinaculum: an anatomic study. *Foot Ankle Int* 1994; 15: 271–275.
- Uğurlu M, Bozkurt M, Demirkale I, Cömert A, Acar HI, Tekdemir I: Anatomy of the lateral complex of the ankle joint in relation to peroneal tendons, distal fibula and talus: a cadaveric study. *Eklem Hastalik Cerrahisi* 2010; 21: 153–158.
- Dangintawat P, Apinun J, Huanmanop T, Agthong S, Chentanez V: New aspect of morphometric study of the superior peroneal retinaculum: pertinent data for surgical repair and reconstruction. *Folia Morphol (Warsz)* 2019.
- Szaro P, Ghali Gataa K, Polaczek M, Ciszek B: The flexor retinaculum connects the surrounding structures into the medial ankle complex. *Appl Sci* 2020; 10: 7972.

25. Lee MH, Chung CB, Cho JH, Mohana-Borges AV, Pretterklieber ML, Trudell DJ *et al.*: Tibialis anterior tendon and extensor retinaculum: imaging in cadavers and patients with tendon tear. *AJR Am J Roentgenol* 2006; 187: W161–168.
26. Zeiss J, Saddemi SR, Ebraheim NA: MR imaging of the peroneal tunnel. *J Comput Assist Tomogr* 1989; 13: 840–844.
27. Guelfi M, Vega J, Malagelada F, Baduell A, Dalmau-Pastor M: Endoscopic treatment of peroneal intrasheath subluxation: a new subgroup with superior peroneal retinaculum injury. *Foot Ankle Int* 2018; 39: 542–550.
28. Rockett MS, Waitches G, Sudakoff G, Brage M: Use of ultrasonography versus magnetic resonance imaging for tendon abnormalities around the ankle. *Foot Ankle Int* 1998; 19: 604–612.
29. Hau WWS, Lui TH, Ngai WK: Endoscopic superior peroneal retinaculum reconstruction. *Arthrosc Tech* 2018; 7: e45–e51.
30. Ersoz E, Tokgoz N, Kaptan AY, Ozturk AM, Ucar M: Anatomical variations related to pathological conditions of the peroneal tendon: evaluation of ankle MRI with a 3D SPACE sequence in symptomatic patients. *Skeletal Radiol* 2019; 48: 1221–1231.
31. Highlander P, Pearson KT, Burns P: Magnetic resonance imaging analysis of peroneal tendon pathology associated with low-lying peroneus brevis muscle belly: a case-control study. *Foot Ankle Spec* 2015; 8: 347–353.
32. Rademaker J, Rosenberg ZS, Beltran J, Colon E: Alterations in the distal extension of the musculus peroneus brevis with foot movement. *AJR Am J Roentgenol* 1997; 168: 787–789.
33. Ozbag D, Gumusalan Y, Uzel M, Cetinus E: Morphometrical features of the human malleolar groove. *Foot Ankle Int* 2008; 29: 77–81.
34. Mabit C, Salanne P, Boncoeur-Martel MP, Fiorenza F, Valleix D, Descottes B *et al.*: [The lateral retromalleolar groove: a radio-anatomic study]. *Bull Assoc Anat (Nancy)* 1996; 80: 17–21.
35. Adachi N, Fukuhara K, Kobayashi T, Nakasa T, Ochi M: Morphologic variations of the fibular malleolar groove with recurrent dislocation of the peroneal tendons. *Foot Ankle Int* 2009; 30: 540–544.